THE JOURNAL OF PHYSICAL CHEMISTRY A

Article

pubs.acs.org/JPCA

The Effect of Water and Bases on the Clustering of a Cyclohexene Autoxidation Product $C_6H_8O_7$ with Sulfuric Acid

Jonas Elm,*[,†] Nanna Myllys,[†] Jan-Niclas Luy,[‡] Theo Kurtén,[¶] and Hanna Vehkamäki[†]

[†]Department of Physics and [¶]Department of Chemistry, University of Helsinki, Finland

[‡]Department of Chemistry, Philipps University, Marburg, Germany

Supporting Information

ABSTRACT: We investigate the molecular interaction between sulfuric acid and a $C_6H_8O_7$ ketodiperoxy acid compound (a proxy for highly oxidized products of, e.g., monoterpene autoxidation) in the presence of water, ammonia, or dimethylamine. The molecular geometries are obtained using density functional theory (M06-2X, PW91, and ωB97X-D) with the 6-31++G(d,p) basis set, and the binding energy is corrected utilizing a high-level DLPNO−CCSD(T)/def2-QZVPP calculation. The formation free energies were calculated (ΔG at 298 K and 1 atm), and the stability of the molecular clusters was evaluated. The presence of bases is found to enhance the interaction between ketodiperoxy acid compounds and sulfuric acid. The addition of $C_6H_8O_7$ compounds to $(H_2SO_4)(NH_3)$ or $(H_2SO_4)((CH_3)_2NH)$ clusters is, however, not able to compete with the corresponding uptake of another sulfuric acid molecule, even at a high loading of organic compounds. We furthermore investigate the origin of the weak binding of peroxyacid compounds using atoms in molecules and natural bonding orbital analysis. The weak binding is caused by an internal hydrogen bond and the lack of a strong hydrogen bond acceptor in the peroxyacid group. These findings indicate that autoxidation products containing solely or mainly hydroperoxide and carbonyl functional groups do not participate in the initial step of new particle formation and thereby only contribute to the growth of atmospheric particles.

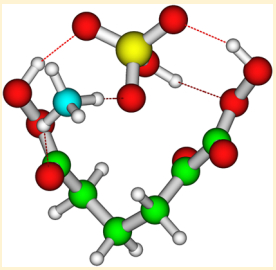

1. INTRODUCTION

The formation of new particles in the atmosphere remains a puzzling phenomenon. Sulfuric acid is known to be a main contributor in many environments,[1] but cannot by itself, or coupled with water, account for new particle formation events observed in the ambient atmosphere.[2,3] Evidence suggests that atmospheric bases efficiently stabilize sulfuric acid clusters via acid−base pairing. The involvement of ammonia, as the most abundant atmospheric base, also yields low new-particle formation rates compared to observations.[2,3] Atmospheric amines such as dimethylamine exhibit a larger stabilization effect than ammonia.[4] and even a few parts per trillion of dimethylamine would be sufficient to account for observed new particle formation events.[5] Resolving the direct involvement of amines in new particle formation is hampered by the sparse amount of continued measurements of amine concentrations. Using a newly developed bisulfate cluster-based atmospheric pressure chemical ionization mass spectrometer for high-sensitivity, no dimethylamine concetrations above 150 ppq were detected during a campaign in Hyytiälä in Spring 2013.[6]

Nonbasic highly oxidized organic compounds formed from oxidation of monoterpenes have been inferred to participate in atmospheric new particle formation, though the structures of the key participating compounds are still unknown.[7−9] It is also unknown at which stage these highly oxidized organic compounds influence the formation of new particles, that is, whether they are only involved in the initial steps in new particle formation,[10] the growth,[11] or contribute to both formation and growth.[12,13]

Highly oxidized organic compounds are likely formed through autoxidation in the atmosphere.[14−17] Following ozonolysis, organic compounds can be oxidized through a series of unimolecular peroxyalkyl radical hydrogen shift reactions and addition of molecular O_2. Savee and Papajak have experimentally directly detected the hydroperoxyalkyl radical product of the peroxyradical hydrogen shift reaction in the oxidation of 1,3-cycloheptadiene.[18] Uni- or bimolecular termination steps yield final closed-shell products with a high oxygen-to-carbon (O/C) ratios of ∼1.[19]

The autoxidation process leads to an array of possible products, mainly containing various carbonyl and hydrogen peroxide moieties. The broad range of potential products hinders the analysis of which compounds participate in the initial steps of the new particle formation. A detailed autoxidation scheme of even the simplest monoterpene α-pinene has still not been identified. The first few steps in the process have recently been elucidated,[19,20] and highly oxidized products such as $C_{10}H_{16}O_9$ have been suggested to form through a peroxy−alkoxy radical route involving a ring-opening reaction.[21] Using the simpler cyclohexene system as a surrogate for larger monoterpene oxidation, Rissanen et al. uncovered the complete autoxidation pathways of the system yielding highly oxidized $C_6H_8O_7$, $C_6H_8O_8$, and $C_6H_8O_9$ compounds.[19] Using the identified highly oxidized $C_6H_8O_7$ ketodiperoxy acid

Received: January 21, 2016
Revised: March 3, 2016
Published: March 8, 2016

DOI: 10.1021/acs.jpca.6b00677
J. Phys. Chem. A 2016, 120, 2240−2249

compound as a proxy for larger monoterpene oxidation products we recently investigated formation free energies of $(H_2SO_4)_{1-2}(C_6H_8O_7)_{1-2}$ clusters using computational methods.[22] We found that the hydrogen peroxyacid moiety binds very weakly to sulfuric acid and that all the formation pathways involving $C_6H_8O_7$ were less favorable than forming a sulfuric acid dimer. This indicates that ketodiperoxy acid autoxidation products cannot be key species in the initial steps of the new particle formation involving sulfuric acid alone. Another stabilizing component such as bases or water might be necessary to yield stable clusters. In this paper, we investigate the effect of bases and water on the stabilization of $(H_2SO_4)_{1-2}(C_6H_8O_7)_{1-2}$ clusters. Using density functional theory (DFT) we obtain the minimum-energy geometries and apply a domain local pair natural orbital coupled cluster (DLPNO−CCSD(T)) method to calculate the binding energies. This study allows for the determination of whether autoxidation products involving peroxyacid groups are capable of entering new particles at the earliest stages or whether the compounds are only involved in the further growth of freshly formed particles.

2. METHODS

2.1. Computational Details. All DFT calculations were performed in Gaussian09, revision B.01,[23] and DLPNO−CCSD(T) calculations were performed in ORCA 3.0.3.[24] The geometries of the $(H_2SO_4)_{1-2}(H_2O)$ and $(H_2SO_4)_{2-3}$ clusters were extracted from the work by Loukonen et al.,[25] and the $(H_2SO_4)_{1-2}(NH_3)$ and $(H_2SO_4)_{1-2}((CH_3)_2NH)$ clusters were taken from the work by Ortega et al.[26] The geometries of the $(H_2SO_4)_{1-2}(C_6H_8O_7)_{1-2}$ clusters are taken by the previous work by Elm et al.[22] The remaining clusters are constructed using a systematic scanning approach that is guided by several thousands of semiempirical (PM6) guess structures and subsequently refined using DFT as previously described.[27−29]

We utilize the DFT functionals M06-2X, PW91, and ωB97X-D, which have previously been identified to perform well in describing clusters of atmospheric relevance.[30−33] All structures are initially evaluated using M06-2X/6-31+G(d), and subsequently all conformers within 3 kcal/mol of the lowest identified structrure are evaluated using M06-2X, PW91, and ωB97X-D with the 6-31++G(d,p) basis set. We recently showed that the reduction from a large 6-311++G(3df,3pd) basis set to the smaller 6-31++G(d,p) basis set had little effect on the thermal contribution to the Gibbs free energy (less than 1 kcal/mol) and did not change the subsequent calculation of the single-point energy substantially.[34] The single-point energies for each functional are then corrected by a high-level ab initio DLPNO−CCSD(T)[35,36] method with a large Def2-QZVPP basis set. The three results are averaged to present the final Gibbs free energies. The advantage of using this approach is that potential errors introduced by a single functional are compensated by the two other calculations. Additionally, the utilization of three functionals simultaneously allows the estimation of the error (depicted as one standard deviation σ) in the calculation arising from the choice of DFT functional. The σ-value thereby represents the sensitivity of the cluster formation reactions to the choice of functional. The DLPNO−CCSD(T)/Def2-QZVPP method has previously been shown to systematically underestimate the binding energies,[37] and the results presented here can thereby be considered as a lower bound. All the thermodynamic parameters were calculated using rigid rotor-harmonic oscillator approximations, at 298.15 K and 1 atm, corresponding to the ground level and lowest part of the troposphere. Note that the results presented here are slightly different from our previous study,[22] as only the 6-31++G(d,p) basis set is used to obtain the geometries in the present work. We will thereby recompute all the values of the $(H_2SO_4)_{1-2}(C_6H_8O_7)_{1-2}$ clusters herein, to allow a direct comparison.

In the bonding pattern analysis of Section 3.6 all calculations were performed using the BP86 functional and a TZVP basis set. Natural bond orbital (NBO) plots were created using ChemCraft.[38] Evaluation of bond critical points in Bader's Quantum Theory of Atoms in Molecules (QTAIM) framework was performed with Multiwfn.[39]

3. RESULTS AND DISCUSSION

3.1. $(C_6H_8O_7)(X)$ Complexes, X = H_2O, NH_3, $(CH_3)_2NH$, and H_2SO_4. We previously calculated the molecular interaction between a $C_6H_8O_7$ ketodiperoxy acid compounds and sulfuric acid.[22] The interaction was found to be weak, with a formation free energy of −0.2 kcal/mol for the $(C_6H_8O_7)(H_2SO_4)$ complex. The calculated Gibbs free energies for forming a complex between the $C_6H_8O_7$ ketodiperoxy acid compound and the common nucleation precursors H_2O, NH_3, $(CH_3)_2NH$, and H_2SO_4 are shown in Table 1.

Table 1. Average Gibbs Free Energy[a] (ΔG, at 298.15 K and 1 atm) for the Formation of the $(C_6H_8O_7)(X)$ Complexes, with X = H_2O, NH_3, $(CH_3)_2NH$, and H_2SO_4

reaction	ΔG	σ
$C_6H_8O_7 + H_2O \leftrightharpoons (C_6H_8O_7)(H_2O)$	5.0	0.7
$C_6H_8O_7 + NH_3 \leftrightharpoons (C_6H_8O_7)(NH_3)$	2.1	0.7
$C_6H_8O_7 + (CH_3)_2NH \leftrightharpoons (C_6H_8O_7)((CH_3)_2NH)$	0.7	0.6
$C_6H_8O_7 + H_2SO_4 \leftrightharpoons (C_6H_8O_7)(H_2SO_4)$	−0.2	0.7

[a]Calculated using DFT/6-31++G(d,p) optimized geometries and a DLPNO−CCSD(T)/def2-QZVPP single-point energy correction. The σ-value depicts one standard deviation. All values are presented in kilocalories per mole.

The $C_6H_8O_7$ compound interacts very weakly with H_2O, NH_3, and $(CH_3)_2NH$, with positive formation free energies in all cases. Water shows the weakest interaction with a Gibbs free energy of formation of 5.0 kcal/mol. The formation free energy is slightly lower for ammonia with ΔG = 2.1 kcal/mol and is found to be most favorable for dimethylamine with ΔG = 0.7 kcal/mol. To calculate the corresponding concentrations of the formed complexes the following general reaction can be considered:

$$C_6H_8O_7 + X \leftrightharpoons (C_6H_8O_7)(X)$$

Assuming mass-balance relations this leads to the following complex concentration at equilibrium:

$$[(C_6H_8O_7)(X)] = [C_6H_8O_7][X]\exp\left(\frac{-\Delta G}{RT}\right)$$

At atmospheric conditions, $[NH_3]$, $[(CH_3)_2NH]$, and $[H_2SO_4]$ are normally in the parts per trillion range ($\sim 1 \times 10^7$ molecules/cm^3), and $[H_2O]$ is roughly $\sim 1 \times 10^{17}$ molecules per cubic centimeter. This would imply that all these complexes have concentrations below 1 molecule per cubic centimeter, illustrating that the concentrations of these two-molecule complexes will be negligible in the ambient atmosphere.

DOI: 10.1021/acs.jpca.6b00677
J. Phys. Chem. A 2016, 120, 2240−2249

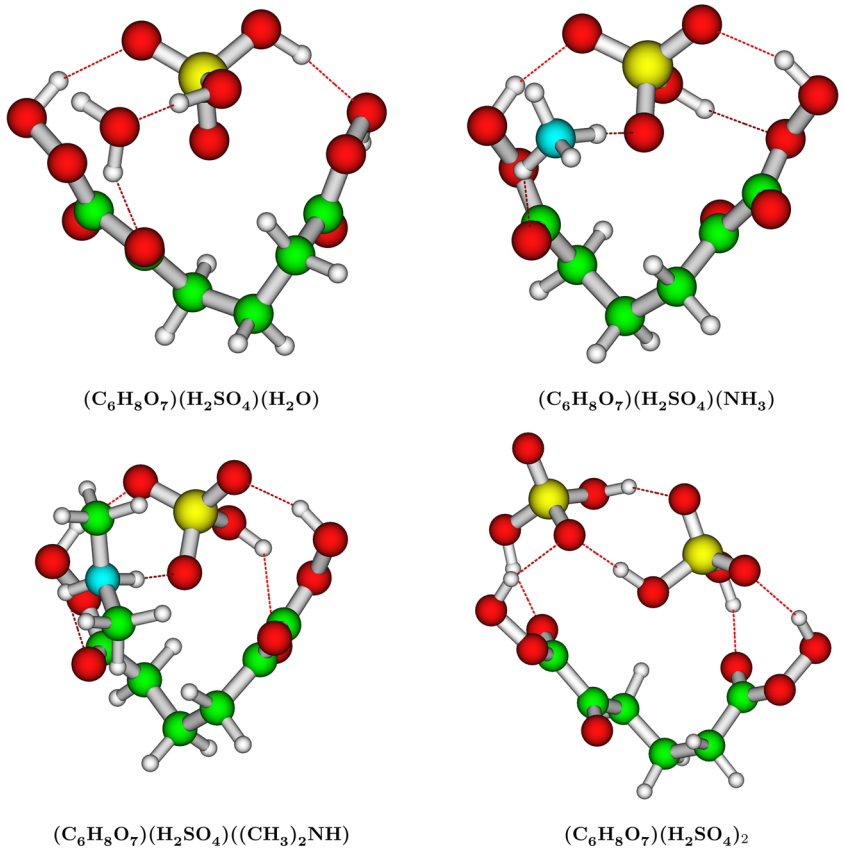

Figure 1. Lowest Gibbs free energy molecular structure of $(C_6H_8O_7)(H_2SO_4)(X)$ clusters, with X = H_2O, NH_3, $(CH_3)_2NH$, and H_2SO_4 calculated at the M06-2X/6-31++G(d,p) level of theory.

Table 2. Average Gibbs Free Energy[a] (ΔG, at 298.15 K and 1 atm) for the Formation of the $(C_6H_8O_7)(H_2SO_4)(X)$ Clusters, with X = H_2O, NH_3, $(CH_3)_2NH$, and H_2SO_4

reaction	ΔG	σ
(1a) $(C_6H_8O_7)(H_2SO_4) + H_2O \leftrightharpoons (C_6H_8O_7)(H_2SO_4)(H_2O)$	−2.5	0.3
(1b) $(C_6H_8O_7)(H_2SO_4) + NH_3 \leftrightharpoons (C_6H_8O_7)(H_2SO_4)(NH_3)$	−8.4	0.3
(1c) $(C_6H_8O_7)(H_2SO_4) + (CH_3)_2NH \leftrightharpoons (C_6H_8O_7)(H_2SO_4)((CH_3)_2NH)$	−18.5	0.8
(1d) $(C_6H_8O_7)(H_2SO_4) + H_2SO_4 \leftrightharpoons (C_6H_8O_7)(H_2SO_4)_2$	−4.8	0.4
(1e) $(H_2SO_4)(H_2O) + C_6H_8O_7 \leftrightharpoons (C_6H_8O_7)(H_2SO_4)(H_2O)$	−1.3	1.0
(1f) $(H_2SO_4)(NH_3) + C_6H_8O_7 \leftrightharpoons (C_6H_8O_7)(H_2SO_4)(NH_3)$	−4.0	0.8
(1g) $(H_2SO_4)((CH_3)_2NH) + C_6H_8O_7 \leftrightharpoons (C_6H_8O_7)(H_2SO_4)((CH_3)_2NH)$	−8.0	0.8
(1h) $(H_2SO_4)_2 + C_6H_8O_7 \leftrightharpoons (C_6H_8O_7)(H_2SO_4)_2$	0.1	0.8
$(H_2SO_4) + H_2O \leftrightharpoons (H_2SO_4)(H_2O)$	−1.4	0.1
$(H_2SO_4) + NH_3 \leftrightharpoons (H_2SO_4)(NH_3)$	−4.6	0.1
$(H_2SO_4) + (CH_3)_2NH \leftrightharpoons (H_2SO_4)((CH_3)_2NH)$	−10.6	0.9
$(H_2SO_4) + H_2SO_4 \leftrightharpoons (H_2SO_4)_2$	−5.2	0.1

[a]Calculated using DFT/6-31++G(d,p) optimized geometries and a DLPNO−CCSD(T)/def2-QZVPP single-point energy correction. The σ-value depicts one standard deviation. H_2SO_4 + X results are shown for comparison. All values are in kilocalories per mole.

Clusters consisting of three components must be considered to further investigate the potential participation of ketodiperoxy acid compounds in the early stages of new particle formation. In the following (Sections 3.2−3.4) we will rely solely on the ΔG values to estimate the cluster stabilities and will look further into the atmospheric implications by taking the concentrations into account in Section 3.5.

3.2. $(C_6H_8O_7)(H_2SO_4)(X)$ Clusters, X = H_2O, NH_3, $(CH_3)_2NH$, and H_2SO_4. The identified lowest Gibbs free energy $(C_6H_8O_7)(H_2SO_4)(X)$ molecular clusters can be seen in Figure 1, calculated at the M06-2X/6-31++G(d,p) level of theory.

The H_2O, NH_3, and $(CH_3)_2NH$ molecules form hydrogen bonds to a vacant carbonyl group in the $C_6H_8O_7$ compound. In the $(C_6H_8O_7)(H_2SO_4)(H_2O)$ cluster the S−OH group of sulfuric acid is found to prefer hydrogen bonding to the water molecule rather than to the peroxyacid group of the $C_6H_8O_7$ compound. The $(C_6H_8O_7)(H_2SO_4)(NH_3)$ and $(C_6H_8O_7)$-$(H_2SO_4)((CH_3)_2NH)$ clusters exhibit a proton transfer from sulfuric acid to the bases. The bases form hydrogen bonds both

DOI: 10.1021/acs.jpca.6b00677
J. Phys. Chem. A 2016, 120, 2240−2249

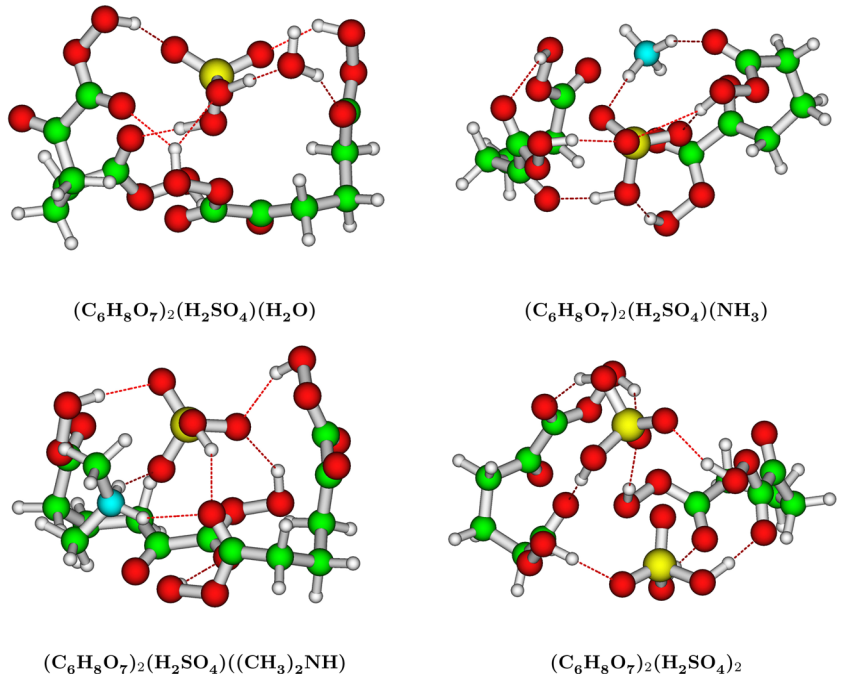

Figure 2. Lowest Gibbs free energy molecular structure of $(C_6H_8O_7)_2(H_2SO_4)(X)$ clusters, with X = H_2O, NH_3, $(CH_3)_2NH$, and H_2SO_4 calculated at the M06-2*X*/6-31++G(d,p) level of theory.

Table 3. Average Gibbs Free Energy[a] (ΔG, at 298.15 K and 1 atm) for the Formation of the $(C_6H_8O_7)_2(H_2SO_4)(X)$ Clusters, with X = H_2O, NH_3, $(CH_3)_2NH$, and H_2SO_4

reaction	ΔG	σ
(2a) $(C_6H_8O_7)_2(H_2SO_4) + H_2O \leftrightharpoons (C_6H_8O_7)_2(H_2SO_4)(H_2O)$	−0.5	0.9
(2b) $(C_6H_8O_7)_2(H_2SO_4) + NH_3 \leftrightharpoons (C_6H_8O_7)_2(H_2SO_4)(NH_3)$	−6.8	1.3
(2c) $(C_6H_8O_7)_2(H_2SO_4) + (CH_3)_2NH \leftrightharpoons (C_6H_8O_7)_2(H_2SO_4)((CH_3)_2NH)$	−17.9	1.1
(2d) $(C_6H_8O_7)_2(H_2SO_4) + H_2SO_4 \leftrightharpoons (C_6H_8O_7)_2(H_2SO_4)_2$	−4.0	0.8
(2e) $(C_6H_8O_7)(H_2SO_4)(H_2O) + C_6H_8O_7 \leftrightharpoons (C_6H_8O_7)_2(H_2SO_4)(H_2O)$	2.2	2.4
(2f) $(C_6H_8O_7)(H_2SO_4)(NH_3) + C_6H_8O_7 \leftrightharpoons (C_6H_8O_7)_2(H_2SO_4)(NH_3)$	1.9	0.6
(2g) $(C_6H_8O_7)(H_2SO_4)((CH_3)_2NH) + C_6H_8O_7 \leftrightharpoons (C_6H_8O_7)_2(H_2SO_4)((CH_3)_2NH)$	0.8	1.7
(2h) $(C_6H_8O_7)(H_2SO_4)_2 + C_6H_8O_7 \leftrightharpoons (C_6H_8O_7)_2(H_2SO_4)_2$	1.0	1.8

[a]Calculated using DFT/6-31++G(d,p) optimized geometries and a DLPNO−CCSD(T)/def2-QZVPP single-point energy correction. The σ-value depicts one standard deviation. All values are in kilocalories per mole.

to the sulfuric acid and the vacant carbonyl group at the peroxyacid group in the $C_6H_8O_7$ compound. In the case of ammonia this indicates that the presence of the $C_6H_8O_7$ compound promotes the proton transfer, which is normally not observed in the $(H_2SO_4)(NH_3)$ complex.[40,41]

The formation of the $(C_6H_8O_7)(H_2SO_4)(X)$ clusters can occur through either a $(C_6H_8O_7)(H_2SO_4)$ + X or a (H_2SO_4)-(X) + $C_6H_8O_7$ mechanism. Table 2 presents the formation free energies for the different cluster-formation pathways.

There is a favorable interaction between the $(C_6H_8O_7)$-(H_2SO_4) complex and the particle precursors H_2O, NH_3, $(CH_3)_2NH$, and H_2SO_4, as shown by reactions (1a−d) in Table 2. This interaction is predominately due to the instability of the $(C_6H_8O_7)(H_2SO_4)$ complex. It is very unlikely that the $(C_6H_8O_7)(H_2SO_4)(X)$ clusters can be formed from the $(C_6H_8O_7)(H_2SO_4)$ complex, as its formation free energy was found to be −0.2 kcal/mol. It is more likely that the $(C_6H_8O_7)(H_2SO_4)(X)$ clusters form through the addition of the $C_6H_8O_7$ compound to the $(H_2SO_4)(X)$ complexes. The addition of $C_6H_8O_7$ to $(H_2SO_4)(H_2O)$ is slightly favorable with a Gibbs free energy of formation of −1.3 kcal/mol as shown in reaction (1e). As the formation free energy of the $(C_6H_8O_7)$-(H_2SO_4) complex is −0.2 kcal/mol, this indicates that water is capable of stabilizing the clustering of $C_6H_8O_7$, in this case by 1.1 kcal/mol, for a single water molecule. The value is very similar to the formation of sulfuric acid monohydrate, for which the corresponding value is −1.4 kcal/mol. The addition of $C_6H_8O_7$ to (H_2SO_4) (NH_3) in reaction (1f) is more favorable with a ΔG value of −4.0 kcal/mol. The formation reaction involving dimethylamine (1g) has a favorable free energy of −8.0 kcal/mol. This indicates that the presence of bases significantly enhances the interaction between ketodiperoxy acid compounds and sulfuric acid. For reaction (1f) the free energy is slightly less favorable than the formation of the sulfuric acid dimer (ΔG = −5.2 kcal/mol). Reaction (1g) is more favorable than the formation of the sulfuric acid dimer, which indicates that $C_6H_8O_7$ compounds could potentially interact thermodynamically favorably with (H_2SO_4)-$((CH_3)_2NH)$ complexes. The reaction free energies are,

DOI: 10.1021/acs.jpca.6b00677
J. Phys. Chem. A 2016, 120, 2240−2249

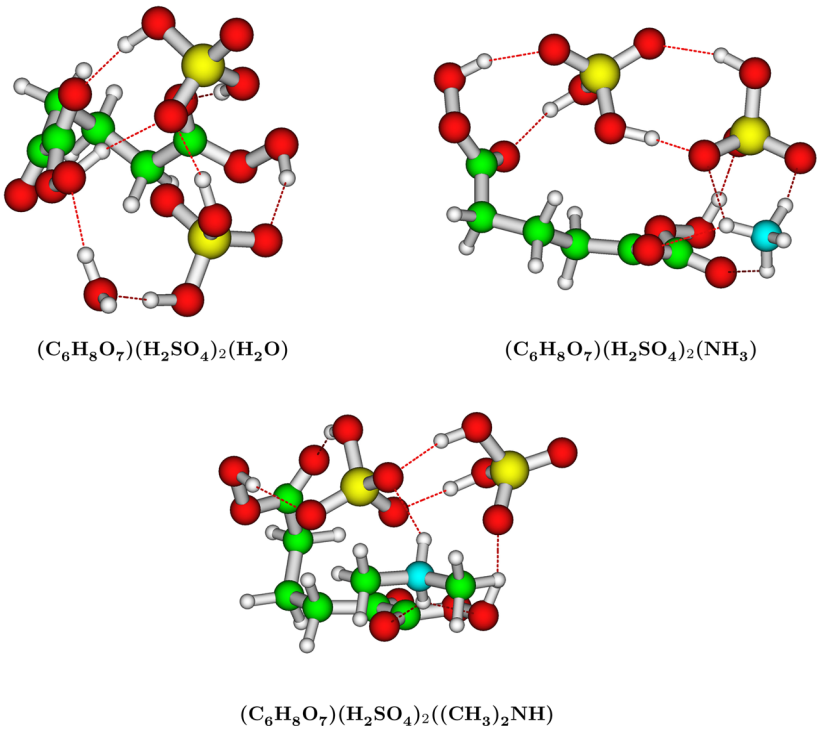

Figure 3. Lowest Gibbs free energy molecular structure of $(C_6H_8O_7)(H_2SO_4)_2(X)$ clusters, with X = H_2O, NH_3, and $(CH_3)_2NH$ calculated at the M06-2*X*/6-31++G(d,p) level of theory.

however, relatively low, and the $C_6H_8O_7$ compound could readily re-evaporate.

3.3. $(C_6H_8O_7)_2(H_2SO_4)(X)$ Clusters, X = H_2O, NH_3, $(CH_3)_2NH$, and H_2SO_4. In Section 3.2 the free energy of reaction forming $(C_6H_8O_7)(H_2SO_4)(X)$ clusters were examined. The inclusion of an additional $C_6H_8O_7$ compound might change the formation pathways, and we here examine clusters with two $C_6H_8O_7$ present, that is, $(C_6H_8O_7)_2(H_2SO_4)(X)$ clusters. The lowest identified Gibbs free energy $(C_6H_8O_7)_2(H_2SO_4)(X)$ molecular clusters can be seen in Figure 2, calculated at the M06-2*X*/6-31++G(d,p) level of theory.

Similarly to the $(C_6H_8O_7)(H_2SO_4)(X)$ clusters, the water, ammonia, and dimethylamine molecules are seen to form hydrogen bonds from the carbonyl group in the peroxyacid moiety to sulfuric acid. Both the $(C_6H_8O_7)_2(H_2SO_4)(NH_3)$ and $(C_6H_8O_7)_2(H_2SO_4)((CH_3)_2NH)$ clusters exhibit a proton transfer. Formation of $(C_6H_8O_7)_2(H_2SO_4)(X)$ clusters can also occur through two different pathways, that is, either though $(C_6H_8O_7)_2(H_2SO_4)$ + X or $(C_6H_8O_7)(H_2SO_4)(X)$ + $C_6H_8O_7$. Table 3 presents the free energies associated with each reaction pathway.

In the same manner as the clusters containing only a single $C_6H_8O_7$ compound, the interaction of $(C_6H_8O_7)_2(H_2SO_4)$ clusters with water, ammonia, and dimethylamine is seen to be favorable. This is again due to the instability of the reactant cluster, which indicates that these clusters will not form through this pathway at atmospherically relevant conditions.

Adding a second $C_6H_8O_7$ compound to the $(C_6H_8O_7)$-$(H_2SO_4)(X)$ clusters is significantly less favorable than the first addition as shown in reaction (2e−h) compared to (1e−h), with free energies in the range of 0.8−2.2 kcal/mol. This is similar in magnitude to the addition of a $C_6H_8O_7$ compound to the $(C_6H_8O_7)(H_2SO_4)$ complex with a value of 0.2 kcal/mol, and it indicates that the enhancing effect of one base/water molecule can only stabilize the addition of a single $C_6H_8O_7$ compound. This is caused by the fact that H_2O, NH_3, and $(CH_3)_2NH$ predominantly interact with a single $C_6H_8O_7$ compound and sulfuric acid, which impairs the beneficial effect of adding a second $C_6H_8O_7$.

Having an additional water/base molecule present could potentially stabilize an additional $C_6H_8O_7$ compound. Possible routes for forming a (2−2−2) clusters could be

$$(a)\ AB \rightarrow OAB \rightarrow OA_2B \rightarrow OA_2B_2 \rightarrow O_2A_2B_2$$

$$(b)\ AB \rightarrow A_2B \rightarrow A_2B_2 \rightarrow OA_2B_2 \rightarrow O_2A_2B_2$$

where A, B, and O refer to sulfuric acid, bases, and organic $C_6H_8O_7$ compounds, respectively. Formation route (a) can easily be excluded, as the initial OAB clusters would not be formed to any significant extent, and the further addition of acid and bases is hindered by the presence of the organic compound (as seen from Table 2 in previous section). In route (b) the organic compounds enter at the later stages, but even the presence of a second base is most likely not sufficient to stabilize (2−2−2) clusters, as it is far more thermodynamically favorable to grow by addition of more sulfuric acid and base molecules.

3.4. $(C_6H_8O_7)(H_2SO_4)_2(X)$ Clusters, X = H_2O, NH_3, and $(CH_3)_2NH$. In this section we examine clusters containing of only a single $C_6H_8O_7$ compound, but with two sulfuric acid molecules present. The lowest Gibbs free energy of the $(C_6H_8O_7)(H_2SO_4)_2(X)$ clusters are presented in Figure 3, calculated at the M06-2*X*/6-31++G(d,p) level of theory.

The molecular interaction between H_2O, NH_3, and $(CH_3)_2NH$ and the $(C_6H_8O_7)(H_2SO_4)_2$ clusters is seen to involve hydrogen bonds between sulfuric acid and the $C_6H_8O_7$ compound. Formation of $(C_6H_8O_7)(H_2SO_4)_2(X)$ clusters can occur through three different pathways: $(C_6H_8O_7)(H_2SO_4)_2$ +

DOI: 10.1021/acs.jpca.6b00677
J. Phys. Chem. A 2016, 120, 2240−2249

Table 4. Average Gibbs Free Energy[a] (ΔG, at 298.15 K and 1 atm) for the Formation of the $(C_6H_8O_7)(H_2SO_4)_2(X)$ Clusters, with X = H_2O, NH_3, $(CH_3)_2NH$, and H_2SO_4

reaction	ΔG	σ
(3a) $(C_6H_8O_7)(H_2SO_4)_2 + H_2O \leftrightharpoons (C_6H_8O_7)(H_2SO_4)_2(H_2O)$	0.7	0.3
(3b) $(C_6H_8O_7)(H_2SO_4)_2 + NH_3 \leftrightharpoons (C_6H_8O_7)(H_2SO_4)_2(NH_3)$	−13.1	0.4
(3c) $(C_6H_8O_7)(H_2SO_4)_2 + (CH_3)_2NH \leftrightharpoons (C_6H_8O_7)(H_2SO_4)_2((CH_3)_2NH)$	−25.5	0.3
(3e) $(H_2SO_4)_2(H_2O) + C_6H_8O_7 \leftrightharpoons (C_6H_8O_7)(H_2SO_4)_2(H_2O)$	1.9	0.6
(3f) $(H_2SO_4)_2(NH_3) + C_6H_8O_7 \leftrightharpoons (C_6H_8O_7)(H_2SO_4)_2(NH_3)$	−0.9	0.9
(3g) $(H_2SO_4)_2((CH_3)_2NH) + C_6H_8O_7 \leftrightharpoons (C_6H_8O_7)(H_2SO_4)_2((CH_3)_2NH)$	−3.6	0.4
(3i) $(C_6H_8O_7)(H_2SO_4)(H_2O) + H_2SO_4 \leftrightharpoons (C_6H_8O_7)(H_2SO_4)_2(H_2O)$	−1.7	0.5
(3j) $(C_6H_8O_7)(H_2SO_4)(NH_3) + H_2SO_4 \leftrightharpoons (C_6H_8O_7)(H_2SO_4)_2(NH_3)$	−9.5	0.2
(3k) $(C_6H_8O_7)(H_2SO_4)((CH_3)_2NH) + H_2SO_4 \leftrightharpoons (C_6H_8O_7)(H_2SO_4)_2((CH_3)_2NH)$	−11.8	0.4
$(H_2SO_4)(H_2O) + H_2SO_4 \leftrightharpoons (H_2SO_4)_2(H_2O)$	−4.9	0.6
$(H_2SO_4)(NH_3) + H_2SO_4 \leftrightharpoons (H_2SO_4)_2(NH_3)$	−12.7	0.2
$(H_2SO_4)((CH_3)_2NH) + H_2SO_4 \leftrightharpoons (H_2SO_4)_2((CH_3)_2NH)$	−16.3	0.8

[a]Calculated using DFT/6-31++G(d,p) optimized geometries and a DLPNO−CCSD(T)/def2-QZVPP single-point energy correction. The σ-value depicts one standard deviation. $(H_2SO_4)(X) + H_2SO_4$ is shown for comparison. All values are in kilocalories per mole.

X, $(H_2SO_4)_2(X) + C_6H_8O_7$, and $(C_6H_8O_7)(H_2SO_4)(X) + H_2SO_4$. The associated Gibbs free energies are presented in Table 4. The free energies of $(H_2SO_4)(X) + H_2SO_4$ reactions are shown for comparison.

The free energy of reaction (3a) is seen to be unfavorable with a Gibbs free energy of 0.7 kcal/mol. The addition of either ammonia or dimethylamine in reaction (3b,c) is once again seen highly favorable due to the instability of the reactant cluster. The addition of a $C_6H_8O_7$ compound to $(H_2SO_4)_2(X)$ clusters in reaction (3e−g) is seen to be unfavorable for the $(H_2SO_4)_2(H_2O)$ cluster, with a ΔG value of 1.9 kcal/mol, but favorable for $(H_2SO_4)_2(NH_3)$ and $(H_2SO_4)_2((CH_3)_2NH)$ clusters with ΔG values of −0.9 and −3.6 kcal/mol, respectively. These values are slightly lower than the corresponding reactions (1e−g), where only a single sulfuric acid is present in the reactant cluster. This indicates that as the clusters grow larger the affinity for adding a $C_6H_8O_7$ compound decreases. This is due to the high stability of the $(H_2SO_4)_2(X)$ reactant cluster. Another formation pathway is the collision of a sulfuric acid molecule with the $(C_6H_8O_7)(H_2SO_4)(X)$ cluster. Here all the formation pathways are seen favorable. The addition of H_2SO_4 to the $(C_6H_8O_7)(H_2SO_4)(H_2O)$ cluster has a slightly negative free energy of −1.7 kcal/mol as seen in reaction (3i). The addition of H_2SO_4 in reaction (3j) is seen to be favorable with a free energy of −9.5 kcal/mol. The corresponding reaction involving dimethylamine is also highly favorable with a free energy of −11.8 kcal/mol. These reaction free energies are however slightly less negative than those of the corresponding reactions without the $C_6H_8O_7$ compound present. This indicates that the presence of a $C_6H_8O_7$ compound in sulfuric acid−base/water clusters would inhibit the further addition of sulfuric acid by up to 4.5 kcal/mol. We also calculated the formation free energies of $(C_6H_8O_7)_2(H_2SO_4)_2(X)$ clusters, with X = H_2O, NH_3, and $(CH_3)_2NH$. The formation paths show similar trends as the above-mentioned cluster formations and will therefore not be further discussed. The reaction free energies of these large clusters are available in the Supporting Information (Table S4).

3.5. Atmospheric Implications. From the previous sections it was found that the interaction of $C_6H_8O_7$ compounds with sulfuric acid is slightly enhanced when a water or base molecule is present. The formation of small $(C_6H_8O_7)(H_2SO_4)(X)$ clusters are observed to be thermodynamically favorable. For these clusters to be relevant under atmospheric conditions the uptake of $C_6H_8O_7$ compound on the $(H_2SO_4)(X)$ complex must compete with the corresponding uptake of another sulfuric acid molecule. We thereby need to consider and compare the following two types of reactions:

$$(H_2SO_4)(X) + C_6H_8O_7 \leftrightharpoons (C_6H_8O_7)(H_2SO_4)(X) \quad (1)$$

$$(H_2SO_4)(X) + H_2SO_4 \leftrightharpoons (H_2SO_4)_2(X) \quad (2)$$

Assuming mass-balance this leads to the following two equilibrium conditions (K_1 and K_2) for reactions (1) and (2), respectively:

$$K_1 = \frac{[(C_6H_8O_7)(H_2SO_4)(X)]}{[(H_2SO_4)(X)][C_6H_8O_7]} \quad (3)$$

$$K_2 = \frac{[(H_2SO_4)_2(X)]}{[(H_2SO_4)(X)][H_2SO_4]} \quad (4)$$

To find the ratio between the concentrations $[(C_6H_8O_7)(H_2SO_4)(X)]$ and $[(H_2SO_4)_2(X)]$, we divide K_1 with K_2 and rearrange:

$$\frac{[(C_6H_8O_7)(H_2SO_4)(X)]}{[(H_2SO_4)_2(X)]} = \frac{K_1}{K_2}\frac{[C_6H_8O_7]}{[H_2SO_4]} = \frac{[C_6H_8O_7]}{[H_2SO_4]}\exp\left(-\frac{\Delta\Delta G}{RT}\right) \quad (5)$$

Here $\Delta\Delta G$ corresponds to the difference in Gibbs free energy between reactions (1) and (2). As seen from Table 2 and Table 3 the $\Delta\Delta G$ value for water, ammonia, and dimethylamine is −3.6, −8.7, and −8.3 kcal/mol, respectively. Taking the exponential $\exp\left(-\frac{\Delta\Delta G}{RT}\right)$ for these values yields 2.3×10^{-3}, 4.2×10^{-7}, and 8.2×10^{-7} at 298 K, respectively. In Table 5 the ratio between $(C_6H_8O_7)(H_2SO_4)(X)$ and $(H_2SO_4)_2(X)$ clusters can be seen at various $[C_6H_8O_7]/[H_2SO_4]$ ratios.

The concentration of sulfuric acid is normally in the range from 1×10^5 to $1 \times 10^7 cm^{-3}$. Assuming a lower limit of the sulfuric acid concentration of 1×10^5 cm^{-3} the ratio between the concentrations $[C_6H_8O_7]/[H_2SO_4]$ in eq 5 would at most be roughly 2 to 3 orders of magnitude during a high loading of

DOI: 10.1021/acs.jpca.6b00677
J. Phys. Chem. A 2016, 120, 2240−2249

Table 5. Concentration Ratio between $(C_6H_8O_7)(H_2SO_4)(X)$ and $(H_2SO_4)_2(X)$ Clusters, with X = H_2O, NH_3, and $(CH_3)_2NH$

$[C_6H_8O_7]/[H_2SO_4]$	ratio: X = H_2O	ratio: X = NH_3	ratio: X = $(CH_3)_2NH$
1:1	2.3×10^{-3}:1	4.2×10^{-7}:1	8.2×10^{-7}:1
10:1	2.3×10^{-2}:1	4.2×10^{-6}:1	8.2×10^{-6}:1
100:1	2.3×10^{-1}:1	4.2×10^{-5}:1	8.2×10^{-5}:1
1000:1	2.3×10^{0}:1	4.2×10^{-4}:1	8.2×10^{-4}:1
10 000:1	2.3×10^{1}:1	4.2×10^{-3}:1	8.2×10^{-3}:1

organic compounds. Using generous values for the concentration of the highly oxidized organic compounds, this implies that $(C_6H_8O_7)(H_2SO_4)(NH_3)$ and $(C_6H_8O_7)(H_2SO_4)((CH_3)_2NH)$ clusters will be present in less than a 1:1000 ratio in the atmosphere compared to $(H_2SO_4)_2(NH_3)$ and $(H_2SO_4)_2((CH_3)_2NH)$ clusters. Even in a high loading of highly oxidized organic compounds and low concentration of sulfuric acid, $C_6H_8O_7$ compounds will not be present in small clusters consisting of sulfuric acid and bases. Note that $(H_2SO_4)_2(NH_3)$ and $(H_2SO_4)_2((CH_3)_2NH)$ clusters will most likely be short-lived as they will probably grow into larger sizes. The ratio between $(C_6H_8O_7)(H_2SO_4)(H_2O)$ and $(H_2SO_4)_2(H_2O)$ clusters is seen to be significantly smaller compared to the base consisting counterparts. This implies that at a high loading of highly oxidized organic compounds compared to the sulfuric acid concentration, the formation of small $(C_6H_8O_7)(H_2SO_4)(H_2O)$ clusters might compete with the formation of the hydrated sulfuric acid dimer. As the sulfuric acid dimer has been shown to be an important step in new particle formation,[42] the formation of $(C_6H_8O_7)(H_2SO_4)(H_2O)$ clusters might potentially hinder the further growth of the clusters. Note that the formation of these $(C_6H_8O_7)(H_2SO_4)(H_2O)$ clusters is also competing with the formation of the sulfuric acid dihydrate cluster $(H_2SO_4)(H_2O)_2$, and water is many orders of magnitude more abundant than organic autoxidation products at atmospheric conditions.

3.6. Bonding Pattern Analysis. We previously suggested that the weak cluster formation potential of peroxyacid compounds originates from the fact that these compounds have an internal hydrogen bond.[22] Furthermore, from the bonding pattern of the $(C_6H_8O_7)(H_2SO_4)$ complex we identified that part of the weak binding originated from the lack of a strong hydrogen bond acceptor in the peroxyacid group. To further quantify the weak bonding of the peroxyacid moiety we compare the simpler formic/acetic peroxyacid to formic/acetic acid. By analyzing the NBOs, we can obtain an indication of the hydrogen bond strength. Figure 4 shows the bonding (bottom orbital of the structures) and antibonding orbitals (top orbital of the structures) involved in the hydrogen bond formation of the acetic acid dimer and peroxy acetic acid dimer. Table 6 shows the corresponding occupation number of the antibonding orbitals.

Table 6. Occupation Number of the Antibonding OH Orbital for Formic/Acetic Acid and Peroxy Formic/Acetic Acid

	antibond occ
FA	0.0145
FA dimer	0.0957
AA	0.0121
AA dimer	0.0964
PFA	0.0364
PFA dimer	0.0327
PAA	0.0441
PAA dimer	0.0357

A good indicator for the dimer formation energy is the occupation of the antibonding OH orbital. It indicates how much electron density is transferred to the opposing oxygen atom and into the hydrogen bond. When the carboxylic acids form dimers the antibonding orbitals exhibits a significant increase in occupation from 0.0145 to 0.0957 and from 0.0121 to 0.0964 for formic acid and acetic acid, respectively. This strengthens the hydrogen bonds and favors dimer formation. In the peroxyacids there is already a comparatively high occupation of the antibonding orbital originating from the formation of an intramolecular hydrogen bond in the monomers. Upon forming the dimer the occupation is lowered indicating a weaker hydrogen bond. It is evident that the intramolecular hydrogen bond present in the peroxyacid moiety reduces the molecule's ability to form dimers or clusters.

To further illustrate the difference in binding strength between the peroxyacids and carboxylic acids, we evaluate the bond critical points at the OH bond, which act as a hydrogen bond donor, and at the hydrogen bond using Bader's QTAIM analysis. Table 7 shows the electron density ($\rho(r)$), Laplacian of the electron density ($\nabla^2\rho(r)$), and the local energy density $H(r)$ for the formation of formic/acetic acid and peroxy formic/acetic acid dimers.

A negative Laplacian ($\nabla^2\rho(r)$) is associated with covalent bonds, while a positive Laplacian indicates a hydrogen bond. The electron density at the bond critical point of the OH bond in formic and acetic acid is seen to decrease from ~0.34 to ~0.29 upon dimer formation. For the peroxyacid compounds there is seen very little change in the electron density at the bond critical point of the O−OH bond when forming the

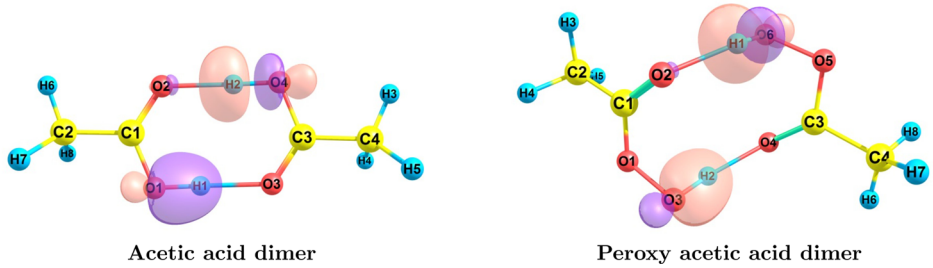

Figure 4. Bonding (bottom) and antibonding (top) orbitals involved in the hydrogen bonds of the acetic acid dimer (left) and the peroxy acetic acid dimer (right).

DOI: 10.1021/acs.jpca.6b00677
J. Phys. Chem. A 2016, 120, 2240−2249

Table 7. QTAIM Analysis of the Electron Density ($\rho(r)$), Laplacian of the Electron Density ($\nabla^2\rho(r)$), and the Local Energy Density $H(r)$ for the Formation of Formic/Acetic Acid and Peroxy Formic/Acetic Acid Dimers

	$\rho(r)$	$\nabla^2\rho(r)$	$H(r)$
FA	0.342	−2.24	−0.624
FA dimer	0.291	−1.76	−0.507
FA dimer	0.0588	0.114	−0.0159
AA	0.344	−2.25	−0.629
AA dimer	0.290	−1.75	−0.505
AA dimer	0.0611	0.117	−0.0171
PFA	0.331	−2.12	−0.597
PFA	0.0345	0.118	−0.000 692
PFA dimer	0.329	−2.16	−0.603
PFA dimer	0.0331	0.109	−0.001 20
PAA	0.327	−2.08	−0.588
PAA	0.0398	0.125	−0.003 04
PAA dimer	0.328	−2.15	−0.600
PAA dimer	0.0345	0.112	−0.001 75

dimer. Similarly, there is seen no change in $\rho(r)$ at the bond critical points, which corresponds to the hydrogen bonds in the peroxyacid compounds. This indicates that the formation free energy for forming the hydrogen bond for the acids should be favorable as electron density is transferred, while there should be no net gain in forming hydrogen bonds for the peroxyacid compounds. This is consistent with the near zero ΔG value obtained for the formation of the $(C_6H_8O_7)(H_2SO_4)$ complex with a value of −0.2 kcal/mol, with a σ-value of 0.7 kcal/mol. This is also reflected in the total local energy ($H(r)$), where the energy of the OH bond increases when a dimer is formed in formic and acetic acid. Contrarily, the energy decreases for the peroxyacids.

Another indicator for the strength of intramolecular hydrogen bonds is the ability of the molecule to donate or accept protons. This can be illustrated by adding either Cl^- for probing the hydrogen bond donor strength or HCl to probe the hydrogen bond acceptor strength and calculating the formation electronic energies (ΔE) of the complexes. Table 8 shows the proton donor and acceptor strengths for formic acid and peroxy formic acid.

Table 8. Hydrogen Bond Donor and Acceptor Strengths[a]

	ΔE
FA	
H-donor	−27.4
H-acceptor	−6.7
PFA	
H-donor	−27.4
H-acceptor	−1.7

[a]Values are presented in kilocalories per mole.

Formic acid and peroxy formic acid have identical hydrogen bond donor strengths with a value of ca. −27.4 kcal/mol. The hydrogen bond acceptor strength is, however, 4 times lower in the case of peroxy formic acid. This further illustrates that the weak clustering ability of the peroxyacid compounds is due to the lack of strong hydrogen bond acceptors as well as the formation of internal hydrogen bonds, as indicated by the NBO and QTAIM analysis.

4. CONCLUSIONS

We have investigated the effect of water, ammonia, and dimethylamine on the clustering between sulfuric acid and a highly oxidized $C_6H_8O_7$ product formed from cyclohexene autoxidation. The free energy for forming a complex between $C_6H_8O_7$ and H_2O, NH_3, $(CH_3)_2NH$, and H_2SO_4 is found to be unfavorable, indicating that only cluster reactions where $C_6H_8O_7$ is added to an existing $(H_2SO_4)(X)$ cluster can have an impact in the atmosphere. We find that the presence of water and bases enhances the interaction between a single ketodiperoxyacid compound and sulfuric acid. Adding another ketodiperoxyacid compound to the cluster is found to be unfavorable in all cases. The addition of sulfuric acid to $(C_6H_8O_7)(H_2SO_4)(X)$ clusters is found to be thermodynamically favorable, but in all cases it is less favorable than the corresponding reaction without the $C_6H_8O_7$ compound present. Assuming equilibrium conditions, it is seen that the addition of $C_6H_8O_7$ compounds to existing clusters is not able to compete with the corresponding uptake of another sulfuric acid molecule, even at a high loading of organic compounds. We find that the origin of the weak clustering of the peroxyacid compound is due to the formation of an internal hydrogen bond and the lack of a strong hydrogen bond acceptor. Note that larger autoxidation products originating from α-pinene oxidation potentially contain additional carbonyl and hydroperoxide groups. The existence of additional functional groups could aid in stabilizing the cluster formation with sulfuric acid by allowing more hydrogen bonds to be formed. The results presented herein should thereby also apply to larger autoxidation products, as highly stabilized clusters should not form unless a strong hydrogen bond acceptor is introduced. These findings lead to the conclusion that autoxidation products containing only peroxyacid, hydroperoxide, and carbonyl groups likely cannot be important species in the initial steps in new-particle formation and thereby can only contribute to aerosol mass in the subsequent growth of freshly nucleated particles. This is further supported by the study by Hao et al.,[43] where ozonolysis products are found to be more involved in the growth of the particles, and OH radical oxidation products are predominantly involved in the initial steps. Most likely oxidation products with several carboxylic acid groups are required to obtain stable clusters and should be further investigated to identify potential key organic species in atmospheric new-particle formation.

■ ASSOCIATED CONTENT

Supporting Information

The Supporting Information is available free of charge on the ACS Publications website at DOI: 10.1021/acs.jpca.6b00677.

All the calculated Gibbs free energies, thermal contribution to the Gibbs free energies, DLPNO−CCSD(T) binding energies, and minimum-energy structures. (PDF)

■ AUTHOR INFORMATION

Corresponding Author

*E-mail: jonas.elm@helsinki.fi. Phone: +45 28938085.

Notes

The authors declare no competing financial interest.

DOI: 10.1021/acs.jpca.6b00677
J. Phys. Chem. A 2016, 120, 2240−2249

■ ACKNOWLEDGMENTS

J.E. thanks the Carlsberg foundation for financial support. We thank the Academy of Finland and ERC Project No. 57360-MOCAPAF for funding and the CSC-IT Center for Science in Espoo, Finland, for computational resources.

■ REFERENCES

(1) Sipilä, M.; Berndt, T.; Petäjä, T.; Brus, D.; Vanhanen, J.; Stratmann, F.; Patokoski, J.; Mauldin, R. L.; Hyvärinen, A.-P.; Lihavainen, H.; et al. The Role of Sulfuric Acid in Atmospheric Nucleation. *Science* **2010**, *327*, 1243−1246.

(2) Kulmala, M.; Vehkamäki, H.; Petäjä, T.; Dal Maso, M.; Lauri, A.; Kerminen, V.-M.; Birmili, W.; McMurry, P. Formation and Growth Rates of Ultrafine Atmospheric Particles: A Review of Observations. *J. Aerosol Sci.* **2004**, *35*, 143−176.

(3) Kirkby, J.; Curtius, J.; Almeida, J.; Dunne, E.; Duplissy, J.; Ehrhart, S.; Franchin, A.; Gagne, S.; Ickes, L.; Kärten, A.; et al. Role of Sulphuric Acid, Ammonia and Galactic Cosmic Rays in Atmospheric Aerosol Nucleation. *Nature* **2011**, *476*, 429−433.

(4) Kurtén, T.; Loukonen, V.; Vehkamäki, H.; Kulmala, M. Amines are Likely to Enhance Neutral and Ion-induced Sulfuric Acid-water Nucleation in the Atmosphere More Effectively than Ammonia. *Atmos. Chem. Phys.* **2008**, *8*, 4095−4103.

(5) Almeida, J.; Schobesberger, S.; Kürten, A.; Ortega, I. K.; Kupiainen-Määttä, O.; Praplan, A. P.; Adamov, A.; Amorim, A.; Bianchi, F.; Breitenlechner, M.; et al. Molecular Understanding of Sulphuric Acid-Amine Particle Nucleation in the Atmosphere. *Nature* **2013**, *502*, 359−363.

(6) Sipilä, M.; Sarnela, N.; Jokinen, T.; Junninen, H.; Hakala, J.; Rissanen, M. P.; Praplan, A.; Simon, M.; Kürten, A.; Bianchi, F.; et al. Bisulfate - Cluster Based Atmospheric Pressure Chemical Ionization Mass Spectrometer for High-Sensitivity (< 100 ppqV) Detection of Atmospheric Dimethyl Amine: Proof-of-concept and First Ambient Data from Boreal Forest. *Atmos. Meas. Tech.* **2015**, *8*, 4001−4011.

(7) Ehn, M.; Thornton, J. A.; Kleist, E.; Sipilä, M.; Junninen, H.; Pullinen, I.; Springer, M.; Rubach, F.; Tillmann, R.; Lee, B.; et al. A Large Source of Low-Volatility Secondary Organic Aerosol. *Nature* **2014**, *506*, 476−479.

(8) Riccobono, F.; Schobesberger, S.; Scott, C. E.; Dommen, J.; Ortega, I. K.; Rondo, L.; Almeida, J.; Amorim, A.; Bianchi, F.; Breitenlechner, M.; et al. Involatile Particles from Rapid Oxidation. *Science* **2014**, *344*, 717−721.

(9) Schobesberger, S.; Junninen, H.; Bianchi, F.; Lönn, G.; Ehn, M.; Lehtipalo, K.; Dommen, J.; Ehrhart, S.; Ortega, I. K.; Franchin, A.; et al. Molecular Understanding of Atmospheric Particle Formation from Sulfuric Acid and Large Oxidized Organic Molecules. *Proc. Natl. Acad. Sci. U. S. A.* **2013**, *110*, 17223−17228.

(10) Zhang, R.; Wang, L.; Khalizov, A. F.; Zhao, J.; Zheng, J.; McGraw, R. L.; Molina, L. T. Formation of Nanoparticles of Blue Haze Enhanced by Anthropogenic Pollution. *Proc. Natl. Acad. Sci. U. S. A.* **2009**, *106*, 17650−17654.

(11) Laaksonen, A.; Kulmala, M.; O'Dowd, C. D.; Joutsensaari, J.; Vaattovaara, P.; Mikkonen, S.; Lehtinen, K. E. J.; Sogacheva, L.; Dal Maso, M.; Aalto, P.; et al. The Role of VOC Oxidation Products in Continental New Particle Formation. *Atmos. Chem. Phys.* **2008**, *8*, 2657−2665.

(12) Riipinen, I.; Yli-Juuti, T.; Pierce, J. R.; Petäjä, T.; Worsnop, D. R.; Kulmala, M.; Donahue, N. M. The Contribution of Organics to Atmospheric Nanoparticle Growth. *Nat. Geosci.* **2012**, *5*, 453−458.

(13) Donahue, N. M.; Ortega, I. K.; Chuang, W.; Riipinen, I.; Riccobono, F.; Schobesberger, S.; Dommen, J.; Baltensperger, U.; Kulmala, M.; Worsnop, D. R.; Vehkamaki, H.; et al. How Do Organic Vapors Contribute to New-particle Formation? *Faraday Discuss.* **2013**, *165*, 91−104.

(14) Crounse, J. D.; Nielsen, L. B.; Jørgensen, S.; Kjaergaard, H. G.; Wennberg, P. O. Autoxidation of Organic Compounds in the Atmosphere. *J. Phys. Chem. Lett.* **2013**, *4*, 3513−3520.

(15) Jokinen, T.; Sipilä, M.; Richters, S.; Kerminen, V.; Paasonen, P.; Stratmann, F.; Worsnop, D.; Kulmala, M.; Ehn, M.; Herrmann, H.; et al. Rapid Autoxidation Forms Highly Oxidized RO2 Radicals in the Atmosphere. *Angew. Chem., Int. Ed.* **2014**, *53*, 14596−14600.

(16) Jokinen, T.; Berndt, T.; Makkonen, R.; Kerminen, V.-M.; Junninen, H.; Paasonen, P.; Stratmann, F.; Herrmann, H.; Guenther, A. B.; Worsnop, D. R.; et al. Production of Extremely Low Volatile Organic Compounds from Biogenic Emissions: Measured Yields and Atmospheric Implications. *Proc. Natl. Acad. Sci. U. S. A.* **2015**, *112*, 7123−7128.

(17) Berndt, T.; Richters, S.; Kaethner, R.; Voigtländer, J.; Stratmann, F.; Sipilä, M.; Kulmala, M.; Herrmann, H. Gas-Phase Ozonolysis of Cycloalkenes: Formation of Highly Oxidized RO2 Radicals and Their Reactions with NO, NO2, SO2, and Other RO2 Radicals. *J. Phys. Chem. A* **2015**, *119*, 10336−10348.

(18) Savee, J. D.; Papajak, E.; Rotavera, B.; Huang, H.; Eskola, A. J.; Welz, O.; Sheps, L.; Taatjes, C. A.; Zádor, J.; Osborn, D. L. Direct Observation and Kinetics of a Hydroperoxyalkyl Radical (QOOH). *Science* **2015**, *347*, 643−646.

(19) Rissanen, M. P.; Kurtén, T.; Sipilä, M.; Thornton, J. A.; Kangasluoma, J.; Sarnela, N.; Junninen, H.; Jørgensen, S.; Schallhart, S.; Kajos, M. K.; et al. The Formation of Highly Oxidized Multifunctional Products in the Ozonolysis of Cyclohexene. *J. Am. Chem. Soc.* **2014**, *136*, 15596−15606.

(20) Rissanen, M. P.; Kurtén, T.; Sipilä, M.; Thornton, J. A.; Kausiala, O.; Garmash, O.; Kjaergaard, H. G.; Petaja, T.; Worsnop, D. R.; Ehn, M.; Kulmala, M.; et al. Effects of Chemical Complexity on the Autoxidation Mechanisms of Endocyclic Alkene Ozonolysis Products: From Methylcyclohexenes toward Understanding αPinene. *J. Phys. Chem. A* **2015**, *119*, 4633−4650.

(21) Kurtén, T.; Rissanen, M. P.; Mackeprang, K.; Thornton, J. A.; Hyttinen, N.; Jørgensen, S.; Kjaergaard, H. G.; Ehn, M. Computational Study of Hydrogen Shifts and Ring-Opening Mechanisms in αPinene Ozonolysis Products. *J. Phys. Chem. A* **2015**, *119*, 11366−11375.

(22) Elm, J.; Myllys, N.; Hyttinen, N.; Kurtén, T. Computational Study of the Clustering of a Cyclohexene Autoxidation Product $C_6H_8O_7$ with Itself and Sulfuric Acid. *J. Phys. Chem. A* **2015**, *119*, 8414−8421.

(23) Frisch, M. J.; Trucks, G. W.; Schlegel, H. B.; Scuseria, G. E.; Robb, M. A.; Cheeseman, J. R.; Scalmani, G.; Barone, V.; Mennucci, B.; Petersson, G. A. et al. *Gaussian 09,* Revision B.01; Gaussian, Inc: Wallingford, CT, 2010.

(24) Neese, F. *WIREs Comput. Mol. Sci.* **2012**, *2*, 73−78.

(25) Loukonen, V.; Kurtén, T.; Ortega, I. K.; Vehkamäki, H.; Pádua, A. A. H.; Sellegri, K.; Kulmala, M. Enhancing Effect of Dimethylamine in Sulfuric Acid Nucleation in the Presence of Water - A Computational Study. *Atmos. Chem. Phys.* **2010**, *10*, 4961−4974.

(26) Ortega, I. K.; Kupiainen, O.; Kurtén, T.; Olenius, T.; Wilkman, O.; McGrath, M. J.; Loukonen, V.; Vehkamäki, H. From Quantum Chemical Formation Free Energies to Evaporation Rates. *Atmos. Chem. Phys.* **2012**, *12*, 225−235.

(27) Elm, J.; Bilde, M.; Mikkelsen, K. V. Influence of Nucleation Precursors on the Reaction Kinetics of Methanol with the OH Radical. *J. Phys. Chem. A* **2013**, *117*, 6695−6701.

(28) Elm, J.; Fard, M.; Bilde, M.; Mikkelsen, K. V. Interaction of Glycine with Common Atmospheric Nucleation Precursors. *J. Phys. Chem. A* **2013**, *117*, 12990−12997.

(29) Elm, J.; Kurtén, T.; Bilde, M.; Mikkelsen, K. V. Molecular Interaction of Pinic Acid with Sulfuric Acid - Exploring the Thermodynamic Landscape of Cluster Growth. *J. Phys. Chem. A* **2014**, *118*, 7892−7900.

(30) Elm, J.; Bilde, M.; Mikkelsen, K. V. Assessment of Density Functional Theory in Predicting Structures and Free Energies of Reaction of Atmospheric Prenucleation Clusters. *J. Chem. Theory Comput.* **2012**, *8*, 2071−2077.

(31) Elm, J.; Bilde, M.; Mikkelsen, K. V. Assessment of Binding Energies of Atmopsheric Clusters. *Phys. Chem. Chem. Phys.* **2013**, *15*, 16442−16445.

DOI: 10.1021/acs.jpca.6b00677
J. Phys. Chem. A 2016, 120, 2240−2249

(32) Leverentz, H. R.; Siepmann, J. I.; Truhlar, D. G.; Loukonen, V.; Vehkamäki, H. Energetics of Atmospherically Implicated Clusters Made of Sulfuric Acid, Ammonia, and Dimethyl Amine. *J. Phys. Chem. A* **2013**, *117*, 3819−3825.
(33) Bork, N.; Du, L.; Kjaergaard, H. G. Identification and Characterization of the HClDMS Gas Phase Molecular Complex via Infrared Spectroscopy and Electronic Structure Calculations. *J. Phys. Chem. A* **2014**, *118*, 1384−1389.
(34) Elm, J.; Mikkelsen, K. V. Computational Approaches for Efficiently Modelling of Small Atmospheric Clusters. *Chem. Phys. Lett.* **2014**, *615*, 26−29.
(35) Riplinger, C.; Neese, F. An Efficient and Near Linear Scaling Pair Natural Orbital Based Local Coupled Cluster Method. *J. Chem. Phys.* **2013**, *138*, doi: 10.1063/1.4773581.
(36) Riplinger, C.; Neese, F. Natural Triple Excitations in Local Coupled Cluster Calculations with Pair Natural Orbitals. *J. Chem. Phys.* **2013**, *139*, doi: 10.1063/1.4821834.
(37) Myllys, N.; Elm, J.; Kurtén, T.; Vehkamäki, H.; Halonen, R. Coupled Cluster Evaluation of the Stability of Atmospheric Acid-Base Clusters with up to 10 Molecules. *J. Phys. Chem. A* **2016**, *120*, 621−630.
(38) http://www.chemcraftprog.com.
(39) Lu, T.; Chen, F. Multiwfn: A multifunctional wavefunction analyzer. *J. Comput. Chem.* **2012**, *33*, 580−592.
(40) Ianni, J. C.; Bandy, A. R. A Density Functional Theory Study of the Hydrates of $NH_3{\cdot}H_2SO_4$ and Its Implications for the Formation of New Atmospheric Particles. *J. Phys. Chem. A* **1999**, *103*, 2801−2811.
(41) Kurtén, T.; Sundberg, M. R.; Vehkamäki, H.; Noppel, M.; Blomqvist, J.; Kulmala, M. Ab Initio and Density Functional Theory Reinvestigation of Gas-Phase Sulfuric Acid Monohydrate and Ammonium Hydrogen Sulfate. *J. Phys. Chem. A* **2006**, *110*, 7178−7188.
(42) Olenius, T.; Kupiainen-Määttä, O.; Ortega, I. K.; Kurtén, T.; Vehkamäki, H. Free Energy Barrier in the Growth of Sulfuric Acid-Ammonia and Sulfuric Acid-Dimethylamine Clusters. *J. Chem. Phys.* 2013, *139*, doi: 10.1063/1.4819024.
(43) Hao, L. Q.; Yli-Pirilä, P.; Tiitta, P.; Romakkaniemi, S.; Vaattovaara, P.; Kajos, M. K.; Rinne, J.; Heijari, J.; Kortelainen, A.; Miettinen, P.; et al. New Particle Formation from the Oxidation of Direct Emissions of Pine Seedlings. *Atmos. Chem. Phys.* **2009**, *9*, 8121−8137.

DOI: 10.1021/acs.jpca.6b00677
J. Phys. Chem. A 2016, 120, 2240−2249